# Evaluation of an active magnetic resonance tracking system for interstitial brachytherapy

Wei Wang[a)]
*Department of Radiology, Brigham and Women's Hospital, Boston, Massachusetts 02115 and Department of Radiation Oncology, Dana-Farber Cancer Institute/Brigham and Women's Hospital, Boston, Massachusetts 02115*

Akila N. Viswanathan and Antonio L. Damato
*Department of Radiation Oncology, Dana-Farber Cancer Institute/Brigham and Women's Hospital, Boston, Massachusetts 02115*

Yue Chen and Zion Tse
*Department of Engineering, The University of Georgia, Athens, Georgia 30602*

Li Pan
*Siemens Healthcare USA, Baltimore, Maryland 21287*

Junichi Tokuda
*Department of Radiology, Brigham and Women's Hospital, Boston, Massachusetts 02115*

Ravi T. Seethamraju
*Siemens Healthcare USA, Boston, Massachusetts 02115*

Charles L. Dumoulin
*Radiology, Cincinnati Children's Hospital Medical Center, Cincinnati, Ohio 45229*

Ehud J. Schmidt
*Department of Radiology, Brigham and Women's Hospital, Boston, Massachusetts 02115*

Robert A. Cormack
*Department of Radiation Oncology, Dana-Farber Cancer Institute/Brigham and Women's Hospital, Boston, Massachusetts 02115*

(Received 6 May 2015; revised 15 October 2015; accepted for publication 30 October 2015; published 23 November 2015)

**Purpose:** In gynecologic cancers, magnetic resonance (MR) imaging is the modality of choice for visualizing tumors and their surroundings because of superior soft-tissue contrast. Real-time MR guidance of catheter placement in interstitial brachytherapy facilitates target coverage, and would be further improved by providing intraprocedural estimates of dosimetric coverage. A major obstacle to intraprocedural dosimetry is the time needed for catheter trajectory reconstruction. Herein the authors evaluate an active MR tracking (MRTR) system which provides rapid catheter tip localization and trajectory reconstruction. The authors assess the reliability and spatial accuracy of the MRTR system in comparison to standard catheter digitization using magnetic resonance imaging (MRI) and CT.

**Methods:** The MRTR system includes a stylet with microcoils mounted on its shaft, which can be inserted into brachytherapy catheters and tracked by a dedicated MRTR sequence. Catheter tip localization errors of the MRTR system and their dependence on catheter locations and orientation inside the MR scanner were quantified with a water phantom. The distances between the tracked tip positions of the MRTR stylet and the predefined ground-truth tip positions were calculated for measurements performed at seven locations and with nine orientations. To evaluate catheter trajectory reconstruction, fifteen brachytherapy catheters were placed into a gel phantom with an embedded catheter fixation framework, with parallel or crossed paths. The MRTR stylet was then inserted sequentially into each catheter. During the removal of the MRTR stylet from within each catheter, a MRTR measurement was performed at 40 Hz to acquire the instantaneous stylet tip position, resulting in a series of three-dimensional (3D) positions along the catheter's trajectory. A 3D polynomial curve was fit to the tracked positions for each catheter, and equally spaced dwell points were then generated along the curve. High-resolution 3D MRI of the phantom was performed followed by catheter digitization based on the catheter's imaging artifacts. The catheter trajectory error was characterized in terms of the mean distance between corresponding dwell points in MRTR-generated catheter trajectory and MRI-based catheter digitization. The MRTR-based catheter trajectory reconstruction process was also performed on three gynecologic cancer patients, and then compared with catheter digitization based on MRI and CT.

**Results:** The catheter tip localization error increased as the MRTR stylet moved further off-center and as the stylet's orientation deviated from the main magnetic field direction. Fifteen catheters'

trajectories were reconstructed by MRTR. Compared with MRI-based digitization, the mean 3D error of MRTR-generated trajectories was $1.5 \pm 0.5$ mm with an in-plane error of $0.7 \pm 0.2$ mm and a tip error of $1.7 \pm 0.5$ mm. MRTR resolved ambiguity in catheter assignment due to crossed catheter paths, which is a common problem in image-based catheter digitization. In the patient studies, the MRTR-generated catheter trajectory was consistent with digitization based on both MRI and CT.
**Conclusions:** The MRTR system provides accurate catheter tip localization and trajectory reconstruction in the MR environment. Relative to the image-based methods, it improves the speed, safety, and reliability of the catheter trajectory reconstruction in interstitial brachytherapy. MRTR may enable in-procedural dosimetric evaluation of implant target coverage.  [http://dx.doi.org/10.1118/1.4935535]

Key words: active tracking, interstitial brachytherapy interventional MRI, treatment planning

## 1. INTRODUCTION

Interstitial brachytherapy involves placement of radioactive sources directly into the tumor through multiple catheters,[1–4] which can be used in the management of a variety of different cancers. In gynecologic brachytherapy, locally advanced cervical cancer is typically treated with intracavitary or interstitial applicators after external beam radiotherapy. Patients with large tumors, vaginal invasion, or adjacent organ (rectum/bladder) invasion often benefit from interstitial catheter placement to improve coverage of the tumor and allow dose escalation. The sharp gradients of radiation dose close to catheters require an appropriate distribution of catheters through the target to achieve an acceptable dosimetric outcome. Image guidance during catheter placement allows for the most precise catheter placement. Transabdominal ultrasound can be used for guiding interstitial catheter placement in gynecologic interstitial implants,[5] and MR guidance has been reported,[4,6] but dosimetric guidance has not been reported.

A major impediment to fast intraprocedural dose calculation is the time needed for catheter trajectory reconstruction. Reconstruction of catheter trajectories after catheter placement determines the available locations for the radioactive sources.[7] Magnetic resonance imaging (MRI) is increasingly used for treatment planning due to the improved visualization of tumors and the surrounding critical organs.[8] International standards for contouring locally advanced cervical cancer rely on MRI.[9,10] However, MRI-based interstitial catheter digitization is challenging because interstitial catheters are identified via MR imaging artifacts (dark contrast) with the MRI sequences used for contouring (e.g., T2-weighted sequence).[11] Although CT or other MRI sequences can be used to aid the reconstruction, image-based catheter digitization suffers from low efficiency and is prone to human errors in catheter identification.[11–15]

Recently, an active MR tracking (MRTR) system was developed by our group to provide accurate and rapid real-time localization of interstitial brachytherapy catheters.[16] It integrates multiple (≥2) receive microcoils into the metallic stylets that are used to advance the catheters into tissue. The microcoil positions are tracked with a dedicated MR sequence. The catheter trajectory can be reconstructed after catheter placement, by continuously tracking the tip position during stylet removal from within the catheter.

In this study, we investigated the performance of the active MRTR system for use in catheter trajectory reconstruction, as compared to standard image-based catheter digitization. The spatial accuracy and reliability in both catheter tip localization and catheter trajectory reconstruction were evaluated. The MRTR system was tested in two phantoms and in three gynecologic cancer patients.

## 2. MATERIALS AND METHODS

### 2.A. Active MRTR system

The active MRTR system is used inside a MR scanner and consists of active MRTR stylets and an 8-channel receiver interface which connects the stylets to the MR scanner's receiver.[16] Each active MRTR stylet consists of two radio-frequency (RF) microcoils attached to a custom-machined ProGuide metallic stylet (Elekta Brachytherapy, Stockholm, Sweden) [Fig. 1(a)]. The MRTR system can acquire the positions ($x$, $y$, and $z$ coordinates) of up to eight microcoils simultaneously by utilizing a dedicated MR tracking sequence described in Ref. 13 (nominal resolution: up to $0.6 \times 0.6 \times 0.6$ mm, update speed: up to 40 Hz). The tracking signals are processed in real time to calculate the instantaneous microcoil locations on the MR scanner's reconstruction computer and then output to an external computer for display. The location of the active stylet tip is acquired by extrapolating a known distance beyond the most distal microcoil along the calculated stylet orientation, which is computed based on the location of the two microcoils.

### 2.B. Catheter tip localization

To investigate the tip localization accuracy, we performed MRTR measurements with active MRTR stylets fixed at different locations and oriented in different directions inside the MR scanner. All the MR experiments in the paper were performed in a 3T MR system (VISIUS iMRI, IMRIS, Winnipeg, MB, Canada).

A cylindrical water phantom (diameter = 50.8 mm, length: 200 mm) was built with a 240-mm-long plastic ProGuide

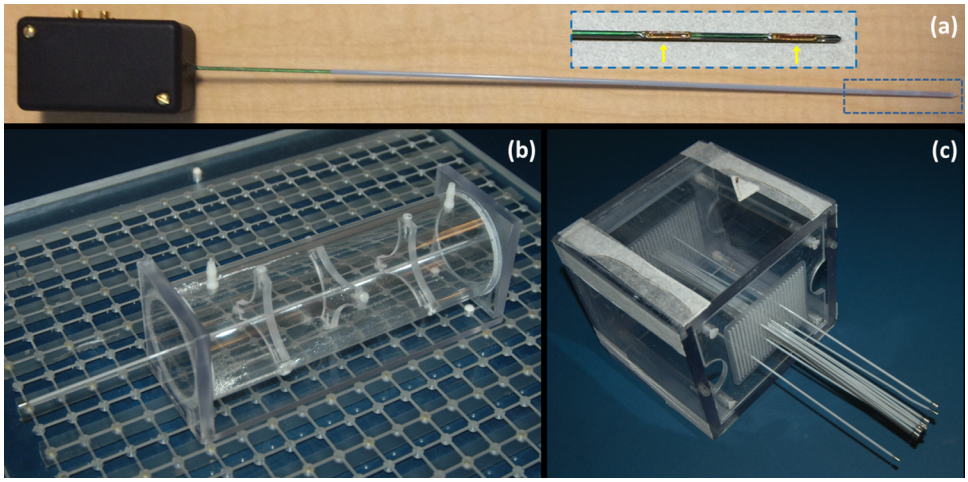


FIG. 1. (a) Photograph of actively tracking brachytherapy catheter, composed of an active MRTR metallic stylet, enclosed by a plastic catheter; the inset figure shows the enlargement (blue dashed box at the tip of the catheter) of the distal portion of the active MRTR stylet. Two flexible printed circuit tracking coils (yellow arrows) were mounted onto the surface of the stylet. The black box at the proximal end was connected to the MR receiver box during MR tracking. (b) Cylindrical water phantom with a catheter fixed through its central axis for catheter tip localization measurements. A template block containing grids of embedded MR visible markers was placed underneath to serve as a coordinate map. (c) Cubic phantom with fifteen catheters inserted with conventional stylets for catheter trajectory reconstruction measurements (agar gel was filled in the phantom for the experiment but not shown in the figure). Thirteen stylets were placed parallel to each other, while one pair crossed each other.

catheter fixed through its central axis [Fig. 1(b)]. The active stylet was fully inserted into the hollow catheter. We define the left-to-right, anterior-to-posterior, and the head-to-foot directions to be $x$-, $y$-, and $z$-axes, respectively, and the isocenter of the magnet to be the origin of the coordinate system. A $500 \times 500$ mm template block containing grids of embedded MR visible markers was placed on the patient bed within the MR scanner, serving as a coordinate map for the $x$–$z$ plane. One of the markers on the template block was set to be at the isocenter of the MRI coordinate frame by using the laser system of the scanner and subsequently confirmed with a high-resolution 3D MR image of the marker.

The water phantom was placed on the template with the active MRTR stylet oriented parallel to main magnetic field $B_0$ (the $z$ axis). While maintaining the same $y$-position ($y = 40$ mm), the tip of the catheter was fixed at seven different locations in the $x$–$z$ plane, ($x = 0$ mm, $z = 0$ mm), ($x = 60$ mm, $z = 0$ mm), ($x = 120$ mm, $z = 0$ mm), ($x = 180$ mm, $z = 0$ mm), ($x = 0$ mm, $z = 60$ mm), ($x = 0$ mm, $z = 120$ mm), and ($x = 0$ mm, $z = 180$ mm). The "ground truth" of each position was measured using a caliper and calculated relative to the isocenter. One hundred MRTR measurements were performed at each phantom location.

For the orientation performance, the phantom was secured at eleven orientations, with the catheter tip at the isocenter of the magnet and the catheter oriented parallel to the $z$ axis, at 15°, 30°, 45°, and 60° from the $z$-axis in the $x$–$z$ plane, and at 15°, 30°, 45°, 60° from the $z$-axis in the $y$–$z$ plane, respectively. The ground truth for each orientation was measured using a protractor. One hundred MRTR measurements were performed at each orientation.

The catheter tip localization error was calculated as the 3D-distance between the tracked catheter tip positions and the ground-truth tip positions.

## 2.C. Catheter trajectory reconstruction

### 2.C.1. Phantom

An agar gel phantom was constructed in a plastic cubic container ($150 \times 150 \times 150$ mm) [Fig. 1(c)]. Two identical plastic templates, labeled the front and back templates with a grid of holes, were mounted at the two opposite sides of the container. A total of fifteen plastic ProGuide catheters were used. Thirteen catheters were inserted parallel to each other, passing through the corresponding holes in the two templates. The other two catheters were used to create a pair of crossing paths, implemented by inserting each catheter from one hole in the front template and exiting through the hole corresponding to the other catheter's insertion hole in the back template.

### 2.C.2. MRTR-based catheter trajectory reconstruction

Catheter trajectory reconstruction experiments were performed during removal of the active stylet from within each catheter. Prior to removal, a short period of static tracking was performed to guarantee precise acquisition of the tip location. A series of (~120–160) points along each catheter's trajectory was acquired in ~3–4 s by continuously tracking the stylet's tip position during its removal.

A MATLAB (Mathworks, Natick, MA) program was written to fit a 3D parametric polynomial curve to the series of positional data for each catheter. The general form of the polynomial to which least squares regression was performed was

$$\begin{cases} x(t) = a_3 t^3 + a_2 t^2 + a_1 t + a_0 \\ y(t) = b_3 t^3 + b_2 t^2 + b_1 t + b_0 \\ z(t) = t \end{cases}. \quad (1)$$

Thereafter, a series of dwell positions $MRTR_{ij}$ ($i = 1, 2,\ldots,15$ designates different catheters, and $j = 1,2,\ldots,N_{MRTRi}$ designates different dwell positions, where $N_{MRTRi}$ is the total number of dwell positions along the $i$th catheter) was calculated at a step size of 2.5-mm distances from the tip position along the fitted 3D catheter curve.

#### 2.C.3. MRI-based catheter digitization

The high-resolution MR images of the phantom were obtained immediately after the tracking experiment using a 3D inversion-recovery gradient-echo (MP-RAGE) sequence (TR/TE/TI = 1200 ms/1.55 ms/900 ms; flip angle $\alpha = 75°$; 5-mm slice, matrix = $312\times384$; FOV = $162\times199$ mm$^2$). The MR image was then imported into a brachytherapy treatment planning system (TPS) (Oncentra, Elekta Brachytherapy, Stockholm, Sweden). Each catheter trajectory was digitized by an experienced brachytherapy physicist, based on the catheter susceptibility artifacts observed on the MR images. The dwell positions $TPS_{ij}$ ($i = 1,2,\ldots,15$ designates catheters, $j = 1,2,\ldots,N_{TPSi}$, where $N_{TPSi}$ is the total number of dwell positions along the $i$th catheter) were calculated with a step size of 2.5 mm from the identified tip position by the planning system.

#### 2.C.4. Comparison of the MRTR-generated trajectories to the MRI-based digitization

MRTR-generated trajectories were compared to those digitized manually on the TPS from the MR images. For each catheter $i$, the catheter error was defined as the distance between the corresponding dwell positions of the MRTR-generated trajectory and the MRI-based digitization,

$$CE_i = \text{mean}_{j=1}^{N_{DW}i} \|MRT_{ij} - TPS_{ij}\|, \quad (2)$$

where $N_{DW_i}$ is the minimum of $N_{MRTRi}$ and $N_{TPSi}$ for the $i$th catheter ($i = 1,2,\ldots,15$ catheters).

For the $i$th catheter, the dwell positions $TPS_{ij}$ ($j = 1, 2,\ldots,N_{TPSi}$) were first spline interpolated and the in-plane offset error of each dwell position $MRTR_{ij}$ was then calculated as the shortest distance $d_{ij}$ from the position $MRTR_{ij}$ to the spline created by $TPS_{ij}$. The in-plane offset error for the $i$th catheter was defined as

$$\Delta_i = \text{mean}_{j=1}^{N_{DW}i}(d_{ij}). \quad (3)$$

The tip error for each catheter was calculated as the distance between the tip dwell position measured from the MRTR reconstructed trajectory and measured from MRI digitization.

### 2.D. Patient study

Catheter placement was performed on three gynecologic cancer patients in the MR scanner on an IRB-approved prospective trial. One patient had recurrent uterine adenocarcinoma and two had cervical cancer (stage IIIB). In each case, 3D T2-weighted images were acquired using a turbo spin echo (TSE) sequence (TR/TE = 3000 ms/104 ms; $\alpha = 120°$; 3-mm slice; matrix = $205\times320$; FOV = $224\times280$ mm$^2$, echo train length = 27). A set of ProGuide interstitial catheters, containing conventional (nonactive tracked) stylets, were inserted through a Syed-Neblett template into the tumor under MRI guidance. In two patients, two conventional stylets were then replaced with the active stylet, and in one patient, four conventional stylets were replaced. After replacement, MRTR was performed continuously during the withdrawal of the active stylet from within the catheter. A smooth parametric cubic curve was then fit to each series of 3D positional data as described in Sec. 2.C.2, prior to data transfer to the TPS system.

After completion of catheter placement in the MRI suite, the patients were transferred to the CT suite for brachytherapy treatment. A CT scan of the patients was acquired (pixel size = $0.6\times0.6$ mm, slice thickness = 1.25 mm) with copper markers inserted in the catheter to enhance their visibility. The CT images were registered to the MR images using a rigid registration algorithm based on catheter positions. CT images were reformatted based on this registration so that the DICOM coordinates of the MR images were used. Catheter digitization was performed on the Oncentra Brachy treatment planning system as described in Sec. 2.C.3 on axial slices of CT and MR images and verified on both sagittal and coronal slices. Note that the CT digitization was based on the copper marker which started 4mm from the catheter tip due to the specifics of the afterloading device and clinical practice. This offset was taken into account in the comparison between MR and CT.

## 3. RESULTS

### 3.A. Catheter tip localization

Figures 2(a) and 2(b) shows the dependence of the mean catheter tip localization errors on the MRTR stylet positions relative to the isocenter of the magnet. The mean MRTR error increased as the MRTR stylet moved further off-center along the $x$-axis and along the $z$-axis. Nevertheless, within an off-center distance of 60 mm, which permitted a 120-mm tracking range along each dimension, the tracking error was less than 0.5 mm.

The mean MRTR error also increased as a function of the angle between the orientation of the stylet and the main magnetic field ($B_0$) direction [Figs. 2(c) and 2(d)]. At angles of up to 60° from the $z$ axis, the errors were all within the resolution limit (0.6 mm). Note that this range of angles is greater than the stylet angulations usually achieved in actual clinical cases.

### 3.B. Catheter trajectory reconstruction

The fifteen catheters' trajectories were successfully reconstructed by active MRTR (Fig. 3). The mean time used to acquire each catheter trajectory was $3.7\pm0.8$ s. The mean 3D catheter error in the fifteen reconstructed trajectories was $1.5\pm0.5$ mm ($d_x = 0.3\pm0.1$ mm; $d_y = 0.3\pm0.1$ mm; $d_z = 1.3\pm0.1$ mm). Results per catheter are summarized in Table I. The mean in-plane error was $0.7\pm0.2$ mm and the mean tip error was $1.7\pm0.5$ mm (Fig. 4).

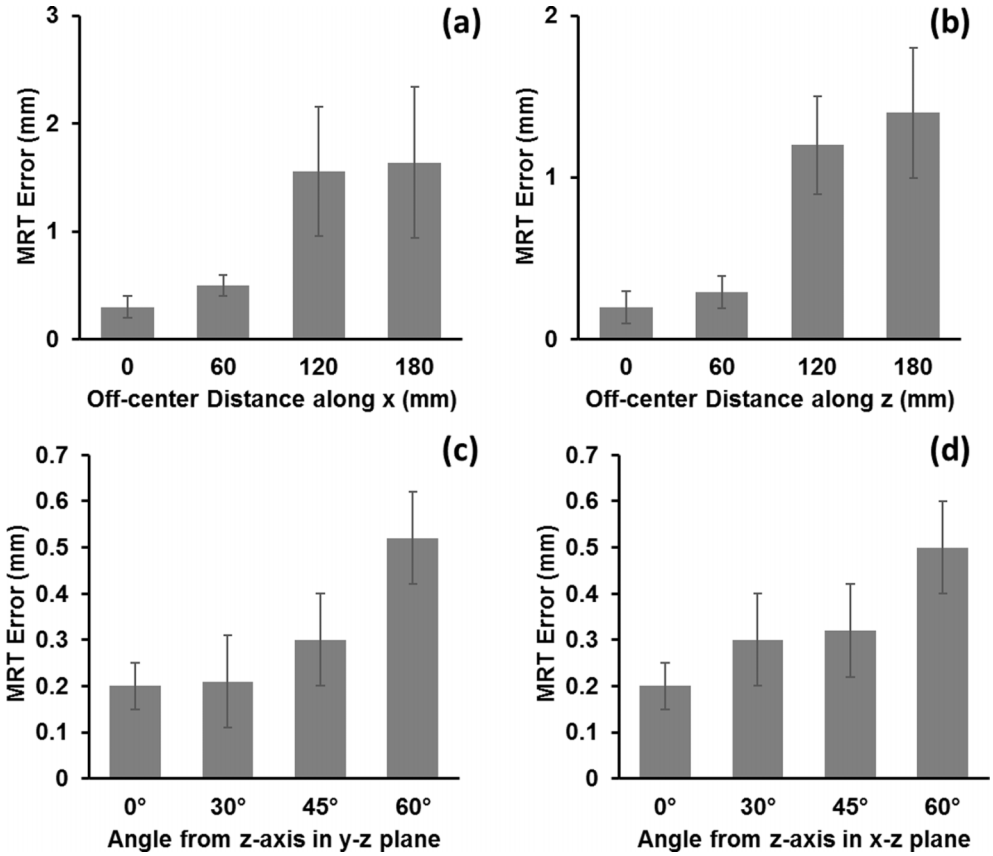


FIG. 2. Mean catheter tip localization error as function of (a) off-center distance along $x$-axis, (b) off-center distance along $z$-axis, (c) angle from the $z$-axis in the $x$–$z$ plane, and (d) angle from the $z$-axis in the $y$–$z$ plane. Two-side error bar represents the standard deviation of the distance error from 100 measurements at each location or orientation.

### 3.C. Patient study

The catheter trajectories were reconstructed from active MRTR performed in the patients. The acquisition time was ~10 s per catheter, allowing ~400 stylet tip positions to be recorded along each catheter trajectory during the stylet removal. The MRTR generated trajectories were compared with those generated on TPS from MR images and CT images, respectively. Trajectories acquired by different methods were highly consistent, as shown in Fig. 5 and Table II.

## 4. DISCUSSION

We evaluated an active MRTR system for brachytherapy catheter localization and trajectory reconstruction in a MR scanner. While there have been reports of use of electromagnetic tracking devices in interstitial brachytherapy,[17,18] this is the first active catheter localization system that is compatible with the MR environment and works in the MR imaging coordinate system without the need for additional registration of the tracking frame of reference to the imaging coordinate system.

GEC-ESTRO guidelines recommend the use of MRI for target and OAR delineation in gynecologic brachytherapy and state that applicator reconstruction is preferably performed in the same image series used for contouring in order to avoid registration uncertainties and patient/organ movement between different image acquisitions.[9,11,19] However, in MRI-based reconstruction, using conventional clinical MR sequences, the catheter/stylet and metal applicator can only be visualized by susceptibility artifacts. The size and shape of the artifacts are not real representations of the catheter/stylet and applicator, and greatly depend on the MR sequence parameters.[11] This makes MRI-based manual reconstruction prone to systematic errors and random errors.[12,20,21] Specifically, in interstitial brachytherapy, the catheter/stylet tip is difficult to identify, which introduces interobserver uncertainty into MRI-based manual catheter identification.[12,22] In contrast, with our MRTR technique, the microcoils are able to receive a strong and unambiguous MR signal which permits a robust localization of the catheter/stylet. Moreover, our MRTR sequence has a built-in mechanism to correct for the static magnetic field $B_0$ and radio-frequency magnetic field $B_1$ inhomogeneities.[16] Hence, this technique is relatively insensitive to systematic error or patient-related errors. In template-based interstitial brachytherapy where placement of a large amount of catheters is required, MRTR can be especially useful in resolving catheters in the setting of ambiguous imaging artifacts, such as when catheters approach or cross each other, because each catheter is individually connected to an independent receiver channel.

Compared with image-based reconstruction methods, MRTR greatly reduces the reconstruction time of catheter trajectories in interstitial brachytherapy. Rather than requiring

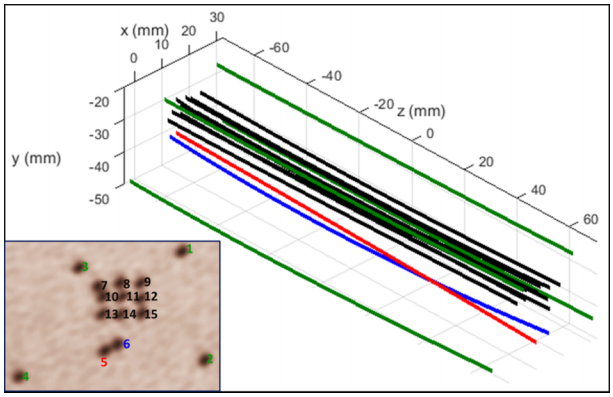


FIG. 3. Fifteen catheter trajectories were acquired by continuously capturing the instantaneous stylet tip positions during active stylet pull-out. The inset figure shows an axial view of the phantom as seen in the brachytherapy treatment planning system with catheter numbering scheme overlaid. Nine catheters (#7–#15) were inserted in a 3×3 grid with a 4 mm spacing at the center, four catheters (#1–#4) close to the four corners of the phantom (with 10-, 15-, 20-, and 25-mm distance to the center, respectively), and a pair of catheters (#5 and #6) with crossed trajectories at approximately 10 mm from the center of template. In all cases, the active tracking system generated stable tracking signal profiles and all the catheter trajectories were resolved without ambiguity.

TABLE I. Catheter errors of the MRTR-generated trajectories along each spatial dimension and in 3D. Data are presented as mean ± standard deviation (SD).

| Catheter number | $d_x$ | $d_y$ | $d_z$ | $d_{3D}$ |
|---|---|---|---|---|
| 1 | 0.2 ± 0.3 | 0.3 ± 0.2 | 1.2 ± 1.0 | 1.6 ± 0.1 |
| 2 | 0.3 ± 0.2 | 0.3 ± 0.2 | 1.2 ± 0.9 | 1.5 ± 0.1 |
| 3 | 0.3 ± 0.3 | 0.2 ± 0.2 | 1.1 ± 0.8 | 1.4 ± 0.1 |
| 4 | 0.1 ± 0.2 | 0.3 ± 0.3 | 0.4 ± 0.3 | 0.6 ± 0.1 |
| 5 | 0.2 ± 0.3 | 0.4 ± 0.3 | 0.9 ± 0.8 | 1.4 ± 0.3 |
| 6 | 0.1 ± 0.1 | 0.2 ± 0.2 | 1.6 ± 1.1 | 2.0 ± 0.3 |
| 7 | 0.2 ± 0.2 | 0.2 ± 0.2 | 1.5 ± 0.2 | 2.0 ± 0.2 |
| 8 | 0.2 ± 0.2 | 0.2 ± 0.2 | 0.3 ± 0.2 | 0.6 ± 0.0 |
| 9 | 0.2 ± 0.2 | 0.3 ± 0.2 | 1.1 ± 0.8 | 1.4 ± 0.1 |
| 10 | 0.3 ± 0.1 | 0.2 ± 0.2 | 1.5 ± 1.0 | 1.9 ± 0.2 |
| 11 | 0.2 ± 0.2 | 0.2 ± 0.2 | 0.5 ± 0.4 | 0.6 ± 0.2 |
| 12 | 0.2 ± 0.1 | 0.2 ± 0.2 | 1.3 ± 0.9 | 1.6 ± 0.1 |
| 13 | 0.2 ± 0.2 | 0.2 ± 0.2 | 0.9 ± 0.7 | 1.1 ± 0.2 |
| 14 | 0.2 ± 0.3 | 0.3 ± 0.2 | 0.9 ± 0.7 | 1.2 ± 0.1 |
| 15 | 0.1 ± 0.2 | 0.2 ± 0.2 | 1.3 ± 1.0 | 1.9 ± 0.1 |
| Mean ± SD | 0.2 ± 0.1 | 0.2 ± 0.1 | 1 ± 0.4 | 1.5 ± 05 |

replacement of the conventional stylets with a tracking device once catheter placement is completed, the MRTR device is implemented in the form of a metallic stylet, which also can be used to drive the catheter into the tissue during insertion. This enables real-time tracking during catheter placement, with high spatial accuracy, as demonstrated in this study, as well as rapid catheter trajectory reconstruction after placement. The fast catheter trajectory reconstruction provided by the MRTR system is well suited for periodic performance of adaptive treatment planning during catheter placement. Future work will focus on using MRTR to provide intraoperative dosimetric feedback of catheter placement to physicians, allowing them to detect tumor regions with dose deficiencies, so that subsequently existing catheter location can be changed and/or additional catheters added as needed. This may result in better dose distribution to the tumor and neighboring OARs, which might reduce tumor recurrence as well as toxicity. These potential therapeutic benefits will require longitudinal evaluation.

In this paper, we studied the effects of MRTR stylet location and orientation on the tip localization accuracy of the MRTR system. The major factor affecting MRTR accuracy is the inhomogeneity of the mean magnetic field ($B_0$) and the nonlinearity of the gradient field, because MRTR inherently depends on the linear relationship between local magnetic field strength and the location inside the magnet. For current MRI scanners, the MR-system-related contributing factor is mainly the gradient nonlinearity, since the systematic $B_0$ inhomogeneity is negligible with proper shimming and the multiplexing acquisition scheme implemented in the MRTR sequence.[23] For our application, there is substantial $B_0$ inhomogeneity in the close proximity of microcoils due to the susceptibility differences between the metallic stylet and surrounding tissue. In the evaluation of our MRTR system performance at different locations inside the MR scanner, tracking accuracy decreased as a function of the off-center distance. This is likely due to the MR gradient nonlinearity which increases significantly in areas farther from the magnet isocenter.[24] Correction methods may be applied in the future if higher precision is required. With regard to orientation dependence of the system, it has been demonstrated that as the orientation of the metallic stylet deviates more from the $B_0$

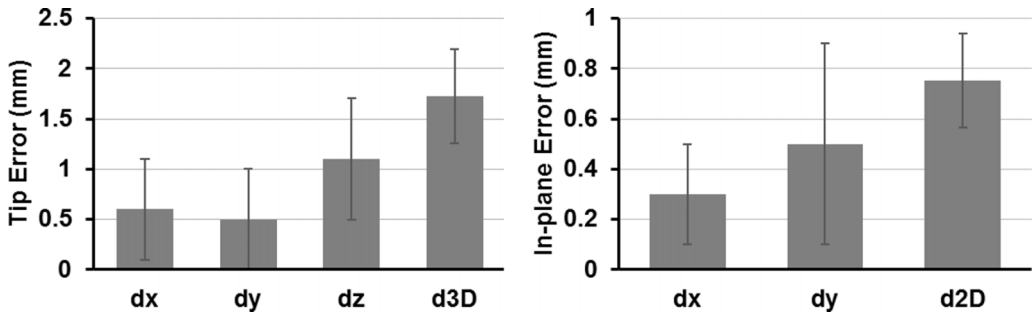


FIG. 4. Left: average tip errors for the catheter trajectory reconstruction of the fifteen catheters. Right: average in-plane errors for the catheter trajectory reconstruction of the fifteen catheters. $|d_x|$, $|d_y|$, and $|d_z|$ are one-dimensional errors along the $x$, $y$, and $z$ axes, respectively. $d_{3D}$ is the 3D distance error and $d_{2D}$ is the in-plane distance error.

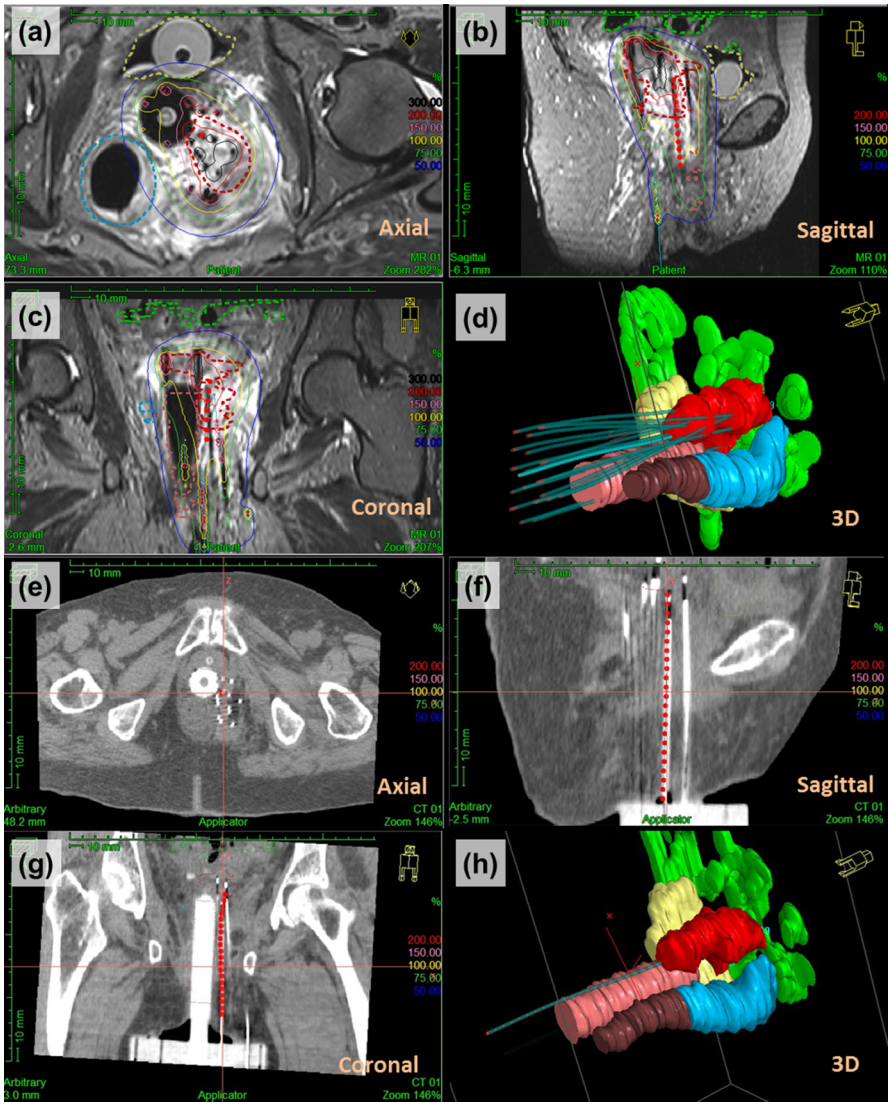


FIG. 5. Catheter trajectory reconstruction on the treatment planning system (Oncentra, Elekta Bracytherapy, Stockholm, Sweden), using MRTR in a patient with recurrent endometrial cancer. [(a)–(c)] Screenshot of one MRTR-generated catheter trajectory (red dots) overlaid on the three orthogonal T2-weighted TSE MR images. Dose distribution is shown as isodose surfaces (solid lines). MRI-based contouring of the tumor and OARs is shown with dashed lines (red: tumor; yellow: bladder; blue: sigmoid; brown: rectum; green: bowel). (d) 3D view of catheter trajectories and geometric volumes representing the tumor and the OARs [organ color code is the same as in (a)–(c)]. The catheter trajectory acquired by MRTR is shown as a highlighted blue cylinder [same trajectory shown as red dots in (a)]. All the other catheters' trajectories are from MRI-based digitization, shown in light blue color. [(e)–(g)] The MRTR generated catheter trajectory (red dot) overlaid on three orthogonal CT images, which was very consistent with the catheter location (bright signal) shown on CT. (h) 3D view of one catheter trajectory digitized from the CT images (light blue cylinder) and the same catheter trajectory extracted from MRTR (red dots).

direction, the disturbed region expands,[25] which may explain the decreased accuracy observed with greater angulation from the $B_0$ direction.

As we quantified the MRTR error by comparing it to MRI-based catheter digitization, the reported error in catheter trajectory reconstruction was a combination of the intrinsic active MRTR error, as described in the previous paragraph, and the MRI-based digitization error. In MRI-based catheter digitization, the imaging artifact size is larger than the physical size of the catheter, and the apparent catheter center is shifted from the real center.[25] Although special MRI sequences have been developed to correct for these errors,[26] we used MR images generated by standard clinical imaging protocols. As compared with digitization based on these MR images, we found the MRTR-generated trajectory had an average 3D error of 1.5 mm, which was mainly a result of error along the $z$ axis. Similar results were obtained when investigating the tip error. The larger $z$-axis errors were partially due to the fact that imaging slice thickness limits digitization accuracy along

TABLE II. Comparison between MRTR-generated catheter trajectories and the image-based digitization (CT and MRI). Equally spaced dwell positions were generated along each trajectory by interpolation, and the corresponding dwell points from the different methods were compared. $d_x$, $d_y$, and $d_z$ represent differences along each axis. $d_{3D}$ represents the 3D distance between corresponding dwell points.

| | $d_x$ (mm) | $d_y$ (mm) | $d_z$ (mm) | $d_{3D}$ (mm) |
|---|---|---|---|---|
| MRTR vs MRI | $0.3 \pm 0.4$ | $-0.1 \pm 0.2$ | $1.3 \pm 0.5$ | $1.5 \pm 0.7$ |
| MRTR vs CT | $0.4 \pm 0.2$ | $-0.6 \pm 0.2$ | $0.2 \pm 0.6$ | $0.7 \pm 0.4$ |

the direction perpendicular to the slice in the image-based methods.

## 5. CONCLUSION

The active MRTR system provides an independent measurement of catheter location in the MR environment and enables MR-based brachytherapy planning of interstitial implants without ionizing radiation. This offers the potential to eliminate the need for a generally time-consuming manual digitization process in the image-based method, or can provide an independent means to verify catheter digitization. The MRTR system is capable of generating catheter trajectories in a time frame that should enable intraprocedural dosimetric evaluation and adaptive planning of interstitial implants in MR guided brachytherapy.

## ACKNOWLEDGMENTS

This work was supported by No. NIH/NCI-R21CA167800, American Heart Association No. 10SDG261039, No. NIH/NIBIB-P41EB015898, University of Georgia-Georgia Regent University seed grant, BWH Department of Radiation Oncology post-doctoral fellowship, and Department of Radiation Oncology/Kaye Family Grant.

[a]Author to whom correspondence should be addressed. Electronic mail: wwang21@partners.org

[1]F. M. Khan and B. J. Gerbi, *Treatment Planning in Radiation Oncology* (Lippincott Williams & Wilkins, Philadelphia, PA, 2007).

[2]C. Polgar, T. Major, J. Fodor, Z. Sulyok, A. Somogyi, K. Lovey, G. Nemeth, and M. Kasler, "Accelerated partial-breast irradiation using high-dose-rate interstitial brachytherapy: 12-year update of a prospective clinical study," Radiother. Oncol. **94**, 274–279 (2010).

[3]Y. Yamada, L. Rogers, D. J. Demanes, G. Morton, B. R. Prestidge, J. Pouliot, G. N. Cohen, M. Zaider, M. Ghilezan, I. C. Hsu, and American Brachytherapy Society, "American Brachytherapy Society consensus guidelines for high-dose-rate prostate brachytherapy," Brachytherapy **11**, 20–32 (2012).

[4]A. N. Viswanathan, J. Szymonifka, C. M. Tempany-Afdhal, D. A. O'farrell, and R. A. Cormack, "A prospective trial of real-time magnetic resonance-guided catheter placement in interstitial gynecologic brachytherapy," Brachytherapy **12**, 240–247 (2013).

[5]S. Mesko, U. Swamy, S. J. Park, L. Borja, J. Wang, D. J. Demanes, and M. Kamrava, "Early clinical outcomes of ultrasound-guided CT-planned high-dose-rate interstitial brachytherapy for primary locally advanced cervical cancer," Brachytherapy **14**, 626–632 (2015).

[6]A. N. Viswanathan, R. Cormack, C. L. Holloway, C. Tanaka, D. O'Farrell, P. M. Devlin, and C. Tempany, "Magnetic resonance-guided interstitial therapy for vaginal recurrence of endometrial cancer," Int. J. Radiat. Oncol., Biol., Phys. **66**, 91–99 (2006).

[7]C. Kirisits, M. J. Rivard, D. Baltas, F. Ballester, M. De Brabandere, R. van der Laarse, Y. Niatsetski, P. Papagiannis, T. P. Hellebust, J. Perez-Calatayud, K. Tanderup, J. L. Venselaar, and F. A. Siebert, "Review of clinical brachytherapy uncertainties: Analysis guidelines of GEC-ESTRO and the AAPM," Radiother. Oncol. **110**, 199–212 (2014).

[8]K. Tanderup, A. N. Viswanathan, C. Kirisits, and S. J. Frank, "Magnetic resonance image guided brachytherapy," Semin. Radiat. Oncol. **24**, 181–191 (2014).

[9]C. Haie-Meder, R. Potter, E. Van Limbergen, E. Briot, M. De Brabandere, J. Dimopoulos, I. Dumas, T. P. Hellebust, C. Kirisits, S. Lang, S. Muschitz, J. Nevinson, A. Nulens, P. Petrow, N. Wachter-Gerstner, and G. E. C. E. W. G. Gynaecological, "Recommendations from Gynaecological (GYN) GEC-ESTRO Working Group (I): Concepts and terms in 3D image based 3D treatment planning in cervix cancer brachytherapy with emphasis on MRI assessment of GTV and CTV," Radiother. Oncol. **74**, 235–245 (2005).

[10]J. C. Dimopoulos, C. Kirisits, P. Petric, P. Georg, S. Lang, D. Berger, and R. Potter, "The Vienna applicator for combined intracavitary and interstitial brachytherapy of cervical cancer: Clinical feasibility and preliminary results," Int. J. Radiat. Oncol., Biol., Phys. **66**, 83–90 (2006).

[11]T. P. Hellebust, C. Kirisits, D. Berger, J. Perez-Calatayud, M. De Brabandere, A. De Leeuw, I. Dumas, R. Hudej, G. Lowe, R. Wills, K. Tanderup, and G. E. C. E. W. G. Gynaecological, "Recommendations from Gynaecological (GYN) GEC-ESTRO Working Group: Considerations and pitfalls in commissioning and applicator reconstruction in 3D image-based treatment planning of cervix cancer brachytherapy," Radiother. Oncol. **96**, 153–160 (2010).

[12]S. Haack, S. K. Nielsen, J. C. Lindegaard, J. Gelineck, and K. Tanderup, "Applicator reconstruction in MRI 3D image-based dose planning of brachytherapy for cervical cancer," Radiother. Oncol. **91**, 187–193 (2009).

[13]N. Milickovic, S. Giannouli, D. Baltas, M. Lahanas, C. Kolotas, N. Zamboglou, and N. Uzunoglu, "Catheter autoreconstruction in computed tomography based brachytherapy treatment planning," Med. Phys. **27**, 1047–1057 (2000).

[14]A. Y. Fung and M. Zaider, "Accuracy in catheter reconstruction in computed tomography planning of high dose rate prostate brachytherapy," Med. Phys. **27**, 2165–2167 (2000).

[15]A. L. Damato, K. Townamchai, M. Albert, R. J. Bair, R. A. Cormack, J. Jang, A. Kovacs, L. J. Lee, K. S. Mak, K. L. Mirabeau-Beale, K. W. Mouw, J. G. Phillips, J. L. Pretz, A. L. Russo, J. H. Lewis, and A. N. Viswanathan, "Dosimetric consequences of interobserver variability in delineating the organs at risk in gynecologic interstitial brachytherapy," Int. J. Radiat. Oncol., Biol., Phys. **89**, 674–681 (2014).

[16]W. Wang, C. L. Dumoulin, A. N. Viswanathan, Z. T. Tse, A. Mehrtash, W. Loew, I. Norton, J. Tokuda, R. T. Seethamraju, T. Kapur, A. L. Damato, R. A. Cormack, and E. J. Schmidt, "Real-time active MR-tracking of metallic stylets in MR-guided radiation therapy," Magn. Reson. Med. **73**, 1803–1811 (2015).

[17]A. L. Damato, A. N. Viswanathan, S. M. Don, J. L. Hansen, and R. A. Cormack, "A system to use electromagnetic tracking for the quality assurance of brachytherapy catheter digitization," Med. Phys. **41**, 101702 (7pp.) (2014).

[18]E. Poulin, E. Racine, D. Binnekamp, and L. Beaulieu, "Fast, automatic, and accurate catheter reconstruction in HDR brachytherapy using an electromagnetic 3D tracking system," Med. Phys. **42**, 1227–1232 (2015).

[19]R. Potter, C. Haie-Meder, E. Van Limbergen, I. Barillot, M. De Brabandere, J. Dimopoulos, I. Dumas, B. Erickson, S. Lang, A. Nulens, P. Petrow, J. Rownd, C. Kirisits, and G. E. W. Group, "Recommendations from Gynaecological (GYN) GEC ESTRO Working Group (II): Concepts and terms in 3D image-based treatment planning in cervix cancer brachytherapy-3D dose volume parameters and aspects of 3D image-based anatomy, radiation physics, radiobiology," Radiother. Oncol. **78**, 67–77 (2006).

[20]K. Tanderup, N. Nesvacil, R. Potter, and C. Kirisits, "Uncertainties in image guided adaptive cervix cancer brachytherapy: Impact on planning and prescription," Radiother. Oncol. **107**, 1–5 (2013).

[21]A. A. De Leeuw, M. A. Moerland, C. Nomden, R. H. Tersteeg, J. M. Roesink, and I. M. Jurgenliemk-Schulz, "Applicator reconstruction and applicator shifts in 3D MR-based PDR brachytherapy of cervical cancer," Radiother. Oncol. **93**, 341–346 (2009).

[22]T. Kapur, J. Egger, A. Damato, E. J. Schmidt, and A. N. Viswanathan, "3-T MR-guided brachytherapy for gynecologic malignancies," Magn. Reson. Imaging **30**, 1279–1290 (2012).

[23]C. L. Dumoulin, S. P. Souza, and R. D. Darrow, "Real-time position monitoring of invasive devices using magnetic resonance," Magn. Reson. Med. **29**, 411–415 (1993).

[24]D. Wang, W. Strugnell, G. Cowin, D. M. Doddrell, and R. Slaughter, "Geometric distortion in clinical MRI systems. Part I: Evaluation using a 3D phantom," Magn. Reson. Imaging **22**, 1211–1221 (2004).

[25]M. E. Ladd, P. Erhart, J. F. Debatin, B. J. Romanowski, P. Boesiger, and G. C. McKinnon, "Biopsy needle susceptibility artifacts," Magn. Reson. Med. **36**, 646–651 (1996).

[26]P. R. Seevinck, H. de Leeuw, C. Bos, and C. J. Bakker, "Highly localized positive contrast of small paramagnetic objects using 3D center-out radial sampling with off-resonance reception," Magn. Reson. Med. **65**, 146–156 (2011).